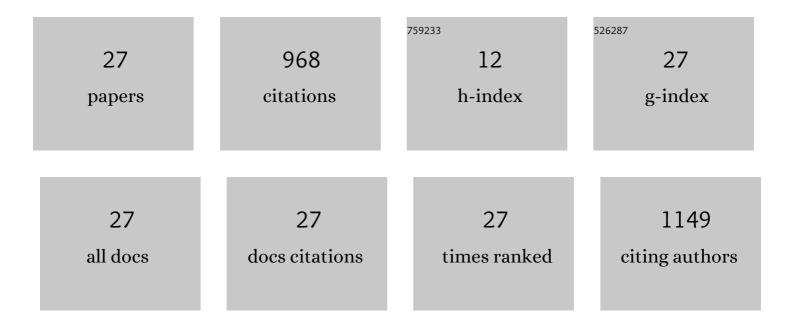
Qing-Song Mei

List of Publications by Year in descending order

Source: https://exaly.com/author-pdf/3876755/publications.pdf Version: 2024-02-01



#	Article	IF	CITATIONS
1	Melting and superheating of crystalline solids: From bulk to nanocrystals. Progress in Materials Science, 2007, 52, 1175-1262.	32.8	504
2	Hall-Petch relations and strengthening of Al-ZnO composites in view of grain size relative to interparticle spacing. Scripta Materialia, 2018, 153, 27-30.	5.2	78
3	Cu/C composites with a good combination of hardness and electrical conductivity fabricated from Cu and graphite by accumulative roll-bonding. Materials and Design, 2016, 110, 124-129.	7.0	50
4	Evolution of microstructure and property of NiTi alloy induced by cold rolling. Journal of Alloys and Compounds, 2015, 653, 156-161.	5.5	40
5	Pressure-induced superheating of Al nanoparticles encapsulated in Al2O3 shells without epitaxial interface. Acta Materialia, 2005, 53, 1059-1066.	7.9	35
6	Cancellous bone-like porous Fe@Zn scaffolds with core-shell-structured skeletons for biodegradable bone implants. Acta Biomaterialia, 2021, 121, 665-681.	8.3	32
7	Cancellous-Bone-like Porous Iron Scaffold Coated with Strontium Incorporated Octacalcium Phosphate Nanowhiskers for Bone Regeneration. ACS Biomaterials Science and Engineering, 2019, 5, 509-518.	5.2	31
8	Fabrication of graphene/copper nanocomposites via in-situ delamination of graphite in copper by accumulative roll-compositing. Composites Part B: Engineering, 2021, 216, 108850.	12.0	31
9	Surface nanocrystallization and property of Ti6Al4V alloy induced by high pressure surface rolling. Surface and Coatings Technology, 2016, 289, 94-100.	4.8	27
10	Production of a high strength Al/(TiAl3+Al2O3) composite from an Al-TiO2 system by accumulative roll-bonding and spark plasma sintering. Materials Science & Engineering A: Structural Materials: Properties, Microstructure and Processing, 2019, 752, 192-198.	5.6	16
11	Gradient microstructure, recrystallization and mechanical properties of copper processed by high pressure surface rolling. Journal of Materials Science and Technology, 2022, 126, 182-190.	10.7	15
12	Different stages in the continuous microstructural evolution of copper deformed to ultrahigh plastic strains. Scripta Materialia, 2012, 67, 1003-1006.	5.2	13
13	Al matrix composites reinforced by high volume fraction of TiAl3 fabricated through combined accumulative roll-bonding processes. Materials Science & Engineering A: Structural Materials: Properties, Microstructure and Processing, 2019, 754, 309-317.	5.6	12
14	Bimodal grain structures and tensile properties of a biomedical Co–20Cr–15W–10Ni alloy with different pre-strains. Rare Metals, 2021, 40, 20-30.	7.1	12
15	Microstructure and mechanical behavior of Al–TiAl3 composites containing high content uniform dispersion of TiAl3 particles. Materials Science & Engineering A: Structural Materials: Properties, Microstructure and Processing, 2020, 786, 139435.	5.6	11
16	Production of Al2O3–Ti2AlN composite with novel combination of high temperature properties. Materials Science & Engineering A: Structural Materials: Properties, Microstructure and Processing, 2014, 607, 6-9.	5.6	8
17	Dependence of Liquid Supercooling on Liquid Overheating Levels of Al Small Particles. Materials, 2016, 9, 7.	2.9	8
18	Production of Surface Layer with Gradient Microstructure and Microhardess on Copper by High Pressure Surface Rolling. Metals, 2020, 10, 73.	2.3	8

QING-SONG MEI

#	Article	IF	CITATIONS
19	Achieving synergistic strengthening and enhanced comprehensive properties of Cu matrix composites at high strength level by incorporating nanocarbons and Al2O3 dual reinforcements. Materials Science & Engineering A: Structural Materials: Properties, Microstructure and Processing, 2022, 839, 142859.	5.6	8
20	GNPs/Al nanocomposites with high strength and ductility and electrical conductivity fabricated by accumulative roll-compositing. Rare Metals, 2021, 40, 2593-2601.	7.1	7
21	Effects of Cold Rolling and Annealing Prior to Dealloying on the Microstructure of Nanoporous Gold. Nanomaterials, 2018, 8, 540.	4.1	6
22	Effect of Squareness of Initial γ′ Precipitates on Creep-Rupture Life of a Ni-Base Single Crystal Superalloy at 760/982°C. Metallurgical and Materials Transactions A: Physical Metallurgy and Materials Science, 2018, 49, 2929-2939.	2.2	5
23	Liquid-phase aluminizing of Ti-6Al-4V with a nanostructured surface layer. Materials Letters, 2017, 193, 169-171.	2.6	3
24	Fabrication and properties of Al-TiAl3-Al2O3 composites with high content of reinforcing particles by accumulative roll-bonding and spark plasma sintering. Materials Today Communications, 2020, 24, 101060.	1.9	3
25	Thermal stability of bimodal grain structure in a cobalt-based superalloy subjected to high-temperature exposure. Rare Metals, 2021, 40, 877-884.	7.1	3
26	Effect of Ion Source Current on the Microstructure and Properties of Cr-DLC Coatings Prepared by Ion Beam-Assisted Arc Ion Plating. Nano, 2017, 12, 1750053.	1.0	1
27	Effect of H2 dilution on the structure and properties of nc-CrC/a-C:H coatings deposited by a hybrid beams system. Nuclear Science and Techniques/Hewuli, 2018, 29, 1.	3.4	1